Liquid Crystals
Publication details, including instructions for authors and subscription information:
http://www.informaworld.com/smpp/title~content=t713926090

Amphiphilic taper-shaped oligomer exhibiting a monolayer smectic A to columnar phase transition

Kazuhito Takeuchi[a]; Yoichi Takanishi[b]; Jun Yamamoto[b]; Atsushi Yoshizawa[a]
[a] Department of Frontier Materials Chemistry, Graduate School of Science and Technology, Hirosaki University, 3 Bunkyo-cho, Hirosaki, Japan [b] Department of Physics, Graduate School of Science, Kyoto University, Oiwake-cho, Kitashirakawa, Sakyo-ku, Kyoto, Japan

Online publication date: 28 May 2010

To cite this Article Takeuchi, Kazuhito , Takanishi, Yoichi , Yamamoto, Jun and Yoshizawa, Atsushi(2010) 'Amphiphilic taper-shaped oligomer exhibiting a monolayer smectic A to columnar phase transition', Liquid Crystals, 37: 5, 507 — 515
To link to this Article: DOI: 10.1080/02678291003611334
URL: http://dx.doi.org/10.1080/02678291003611334

Liquid Crystals,
Vol. 37, No. 5, May 2010, 507–515

Taylor & Francis
Taylor & Francis Group

Amphiphilic taper-shaped oligomer exhibiting a monolayer smectic A to columnar phase transition

Kazuhito Takeuchi[a], Yoichi Takanishi[b], Jun Yamamoto[b] and Atsushi Yoshizawa[a]*

[a]*Department of Frontier Materials Chemistry, Graduate School of Science and Technology, Hirosaki University, 3 Bunkyo-cho, Hirosaki 036-8561, Japan;* [b]*Department of Physics, Graduate School of Science, Kyoto University, Oiwake-cho, Kitashirakawa, Sakyo-ku, Kyoto 606-8562, Japan*

(*Received 18 October 2009; final version received 11 January 2010*)

We prepared two series of liquid-crystalline oligomers composed of phenylpyrimidine based mesogenic cores, alkyl spacers and semiperfluorinated alkyl chains in one series and only alkyl chains in the second series. Their physical properties were investigated using optical microscopy, differential scanning calorimetry and X-ray diffraction measurements. The oligomers possessing a semiperfluorinated alkyl chain show a phase sequence of SmC–SmA–Col when the number of phenylpyrimidine moieties was increased. The compound possessing three phenylpyrimidine cores was found to exhibit monolayer SmA and Col phases. On the other hand, the oligomer composed of an alkyl chain and three phenylpyrimidine cores showed only a nematic phase. We discuss effects of the shape amphiphilicity and the hydrocarbon–fluorocarbon amphiphilicity on phase transition behaviour of the amphiphilic oligomers.

Keywords: liquid crystals; phase transition; amphiphilicity; oligomer

1. Introduction

Supermolecular assemblies with well-defined morphologies (e.g. layers, interpenetrating networks, columns, and spheroids) are fundamental components for structure formation in biological systems, as well as for application in the production of novel functional materials. For those reasons, investigation of the driving forces of this self-assembly process of liquid-crystalline materials is an important contemporary research topic [1–18]. A primary characteristic in the thermotropic liquid crystal phases is the gross molecular shape of a compound [19, 20]. Well-designed intermolecular interactions, e.g. metal-containing systems [21, 22], charge-transfer systems [23], and hydrogen-bonded systems [6, 7, 24] have been investigated. Furthermore, molecular topology [1] and microsegregation [3, 4] have attracted much attention as origins for producing novel self-organising systems. Marked differences exist in phase transition behaviour between lyotropic and thermotropic liquid crystals. The mesophase morphologies of the lyotropic liquid crystals are governed mainly by the volume fraction of two incompatible segments combined in such molecules. The phase sequence of lamellar (smectic, SmA), bicontinuous cubic (Cub_v), hexagonal columnar (Col_h), and micellar cubic (Cub_I) upon increasing the volume fraction of one component is typical for morphologies of mesophases of these systems. Amphiphilic thermotropic liquid crystals that show such a lyotropic phase sequence have attracted much attention. The value of the interface curvature between hydrophilic regions and lipophilic regions is recognised as the key factor determining the mesophase morphology of these systems. Recently, we prepared amphiphilic liquid-crystalline oligomers **1a**–**1c** that comprise cyanobiphenyl mesogenic moieties and a semiperfluorinated alkyl chain. Results of that study showed an unusual phase sequence of lamellar-columnar-bicontinuous cubic phases when the number of cyanobiphenyl moieties was increased, as shown in Figure 1 [25]. In fact, X-ray diffractometry measurements of compound **1c** suggest that the SmA phase has an undulating layer structure. Competition of two different molecular packings might give rise to that fluctuation: (a) a segregation effect attributable to incompatibility between a semiperfluorinated moiety and cyanobiphenyl mesogens; and (b) a steric effect attributable to a pronounced taper shape of compound **1c** [25]. The fluctuated lamellar structure in the SmA phase of compound **1c** is thought to be stabilised by antiparallel dipole–dipole interactions between the cyanobiphenyl groups in adjacent layers [26]. Figure 2 portrays a schematic illustration of the fluctuated SmA to bicontinuous cubic phase.

For this study, we prepared amphiphilic liquid-crystalline oligomers **2a**–**2c** that comprise phenylpyrimidine moieties and a semiperfluorinated alkyl chain (Figure 3). We report herein the phase transition behaviour of compounds **2a**–**2c**. The liquid-crystalline oligomers have hydrocarbon–fluorocarbon amphiphilicity that prefers a segregated structure and the shape amphiphilicity that prefers a monolayer structure. The hydrocarbon-fluorocarbon amphiphilicity decreases, whereas the shape amphiphilicity increases from

*Corresponding author. Email: ayoshiza@cc.hirosaki-u.ac.jp

ISSN 0267-8292 print/ISSN 1366-5855 online

DOI: 10.1080/02678291003611334
http://www.informaworld.com

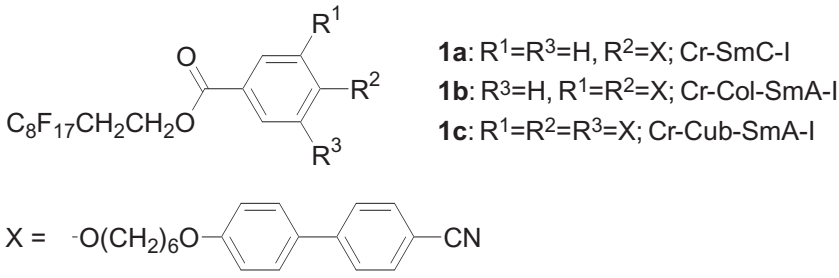

Figure 1. Molecular structures and phase sequences of compounds **1a**–**1c**.

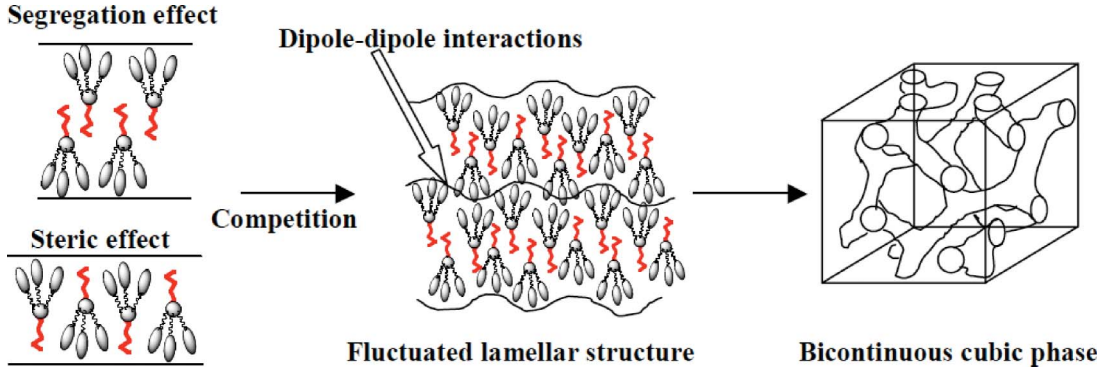

Figure 2. Schematic illustration of the fluctuated SmA to bicontinuous cubic phase of compound **1c**.

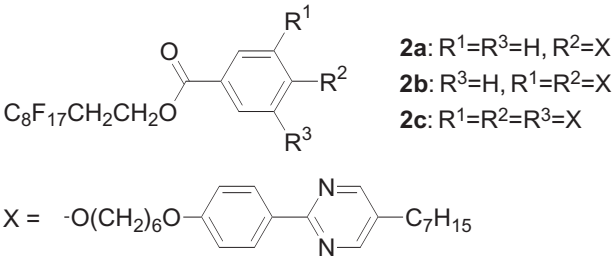

Figure 3. Molecular structures of compounds **2a**–**2c**.

compound **2a** to compound **2c**. We discuss effects of the two different amphiphilicities on the phase structure of the liquid-crystalline oligomers.

2. Experimental

2.1 Spectroscopic analysis

The purities of all final compounds were checked using HPLC (JAIGEL-1H column, LC9101; Japan Analytical Industry Co. Ltd., Tokyo, Japan). Chloroform was used as eluent. Detection of products was achieved using UV irradiation ($\lambda = 254$ nm). These were also checked using elemental analysis (EA. 1110; CE Instruments Ltd., Hercules, USA).

Infrared (IR) spectroscopy (FTS-30; Bio-Rad Laboratories, Inc., Wigan, UK) and proton nuclear magnetic resonance (^{1}H NMR) spectroscopy (JNM-GX270, JNM-A400 or JNM-ECA500; JEOL, Akishima, Japan) elucidated the structures of the final products.

2.2 Preparation of materials

2.2.1 2-[4-(6-Bromohexyloxy)phenyl]-5-heptylpyrimidine

2-(4-Hydroxyphenyl)-5-heptylpyrimidine (0.88 g, 3.3 mmol) and 1,6-dibromohexane (1.7 g, 4.5 mmol) were dissolved in cyclohexanone (20 ml). Potassium carbonate (0.46 g, 3.3 mmol) was added; the resulting mixture was stirred at 75°C for 8 h. The reaction mixture was filtered and the solvent removed by evaporation under reduced pressure. The residue was purified using column chromatography on silica gel with dichloromethane as eluent. Recrystallisation from hexane gave the desired product: yield 0.91 g (64%) of a white solid. ^{1}H NMR (500 MHz, $CDCl_3$) δ_H/ppm: 8.57 (s, 2H, Ar-**H**), 8.35 (d, 2H, Ar-**H**, $J = 9.2$ Hz), 6.98 (d, 2H, Ar-**H**, $J = 9.2$ Hz), 4.03 (t, 2H, -OC**H$_2$**-, $J = 6.3$ Hz), 3.43 (t, 2H, BrC**H$_2$**-, $J = 6.9$ Hz), 2.59 (t, 2H, Ar-C**H$_2$**-, $J = 7.5$ Hz), 1.90 (qui, 2H, aliphatic-**H**, $J = 6.9$ Hz), 1.83 (qui, 2H, aliphatic-**H**, $J = 6.9$ Hz), 1.64 (qui, 2H, aliphatic-**H**, $J = 7.5$ Hz), 1.52 (qui, 4H, aliphatic-**H**, $J = 3.7$ Hz), 1.34–1.27 (m, 8H, aliphatic-**H**), 0.88 (t, 3H, -C**H$_3$**, $J = 6.9$ Hz); IR (KBr) ν_{max}/cm^{-1}: 2931, 2855, 1605, 1582, 1250, 1170 cm^{-1}.

2.2.2 Ethyl 4-{6-[4-(5-heptylpyrimidin-2-ly) phenyloxy]hexyloxy}benzoate

First, 2-[4-(6-bromohexyloxy)phenyl]-5-heptylpyrimidine (0.39 g, 0.89 mmol) and ethyl 4-hydroxybenzoate (0.15 g, 0.89 mmol) were dissolved in cyclohexanone (20 ml). Then, K_2CO_3 (0.15 g, 1.0 mmol) was added and the resulting mixture was stirred at 130°C for 10 h. The reaction mixture was filtered and the solvent removed by evaporation under reduced pressure. The residue was purified using column chromatography on silica gel with a toluene/ethyl acetate (20/1) mixture as eluent and recrystallisation from a hexane/ethanol (1/3) mixture: yield 0.40 g (86%) of a white solid. ^{1}H NMR (500 MHz, $CDCl_3$) δ_H/ppm: 8.57 (s, 2H, Ar-**H**), 8.34 (d, 2H, Ar-**H**, $J = 8.6$ Hz), 7.99 (d, 2H, Ar-**H**, $J = 9.2$ Hz), 6.98 (d, 2H, Ar-**H**, $J = 9.2$ Hz), 6.90 (d, 2H, Ar-**H**, $J = 9.2$ Hz), 4.34 (qua, 2H, -COOC**H$_2$**-, $J = 7.0$ Hz), 4.05 (t, 2H, -OC**H$_2$**-, $J = 6.3$ Hz), 4.03 (t, 2H, -OC**H$_2$**-, $J = 6.3$ Hz), 2.60 (t, 2H, Ar-C**H$_2$**-, $J = 7.5$ Hz), 1.86–1.84 (m, 4H, aliphatic-**H**), 1.64 (qui, 2H, aliphatic-**H**, $J = 7.5$ Hz), 1.57 (qui, 4H, aliphatic-**H**, $J = 3.5$ Hz), 1.39–1.24 (m, 11H, aliphatic-**H**), 0.88 (t, 3H, -C**H$_3$**, $J = 6.9$ Hz); IR (KBr) ν_{max}/cm^{-1}: 2943, 2867, 1719, 1606, 1583, 1251, 1169 cm^{-1}.

2.2.3 4-{6-[4-(5-Heptylpyrimidin-2-ly) phenyloxy]hexyloxy}benzoic acid

Ethyl 4-{6-[4-(5-heptylpyrimidin-2-ly)phenyloxy]hexyloxy}benzoate (0.38 g, 0.72 mmol) was added to a solution of KOH (0.15 g, 2.5 mmol) in an ethanol– water (10:1) mixture (10.5 ml). The resulting solution was refluxed for 4 h. The solution was acidified with aq. HCl. The solution was extracted with dichloromethane. The organic layers were combined, dried over magnesium sulphate, filtered, and evaporated. The product was washed with ethanol: yield 0.29 g (81%) of a white solid. ^{1}H NMR (500 MHz, $CDCl_3$) δ_H/ppm: 8.59 (s, 2H, Ar-**H**), 8.34 (d, 2H, Ar-**H**, $J = 8.6$ Hz), 8.06 (d, 2H, Ar-**H**, $J = 9.2$ Hz), 6.99 (d, 2H, Ar-**H**, $J = 8.6$ Hz), 6.94 (d, 2H, Ar-**H**, $J = 9.2$ Hz), 4.05 (t, 4H, -OC**H$_2$**-, $J = 6.3$ Hz), 2.60 (t, 2H, Ar-C**H$_2$**-, $J = 7.5$ Hz), 1.86 (qui, 4H, aliphatic-**H**, $J = 6.9$ Hz), 1.64 (qui, 2H, aliphatic-**H**, $J = 7.5$ Hz), 1.58 (qui, 4H, aliphatic-**H**, $J = 3.8$ Hz), 1.35–1.28 (m, 8H, aliphatic-**H**), 0.88 (t, 3H, -C**H$_3$**, $J = 6.9$ Hz); IR (KBr) ν_{max}/cm^{-1}: 2928, 2851, 1696, 1607, 1581, 1254, 1167 cm^{-1}.

*2.2.4. 1H,1H,2H,2H-Heptadecafluoro-1-decyl 4-{6-[4-(5-heptylpyrimidin-2-ly)phenyloxy]hexyloxy} benzoate, (**2a**)*

To a solution of 4-{6-[4-(5-heptylpyrimidin-2-ly)phenyloxy]hexyloxy}benzoic acid (0.25 g, 0.53 mmol) and 1H, 1H, 2H, 2H-heptadecafluoro-1-decanol (0.25 g, 0.54 mmol) in dichloromethane (20 ml), *N, N′*-dicyclohexylcarbodiimide (0.14 g, 0.65 mmol) and 4-(*N, N*-dimethylamino)pyridine (7.7 mg, 0.065 mmol) were added. The resulting solution was stirred at room temperature for 21 h. Precipitated materials were removed by filtration. After removal of the solvent by evaporation, the residue was purified using column chromatography on silica gel with a toluene/ethyl acetate (5/1) mixture as eluent. Recrystallisation from an ethanol/ethyl acetate (1/1) mixture gave the desired product: yield 0.18 g (38%) of a white solid. ^{1}H NMR (500 MHz, $CDCl_3$) δ_H/ppm: 8.57 (s, 2H, Ar-**H**), 8.34 (d, 2H, Ar-**H**, $J = 8.6$ Hz), 7.98 (d, 2H, Ar-**H**, $J = 9.2$ Hz), 6.98 (d, 2H, Ar-**H**, $J = 9.2$ Hz), 6.92 (d, 2H, Ar-**H**, $J = 9.2$ Hz), 4.60 (t, 2H, -COOC**H$_2$**-, $J = 6.3$ Hz), 4.05 (t, 2H, -OC**H$_2$**-, $J = 6.3$ Hz), 4.04 (t, 2H, -OC**H$_2$**-, $J = 6.3$ Hz), 2.65–2.55 (m, 4H, aliphatic-**H**), 1.86 (qui, 4H, aliphatic-**H**, $J = 6.9$ Hz), 1.64 (qui, 2H, aliphatic-**H**, $J = 7.5$ Hz), 1.60–1.54 (m, 4H, aliphatic-**H**), 1.35–1.28 (m, 8H, aliphatic-**H**), 0.88 (t, 3H, -C**H$_3$**, $J = 6.9$ Hz); IR (KBr) ν_{max}/cm^{-1}: 2941, 2856, 1718, 1608, 1585, 1254, 1149, 1204 cm^{-1}. Elemental analysis, calculated for $C_{40}H_{41}N_2O_4F_{17}$: C, 51.29%; H, 4.41%; N, 2.99%. Found: C, 51.49%; H, 4.56%; N, 2.98%.

*2.2.5 1H,1H,2H,2H-Heptadecafluoro-1-decyl 3,4-bis{6-[4-(5-heptylpyrimidin-2-ly)phenyloxy] hexyloxy}benzoate, (**2b**)*

Synthesised using the same method as that used for compound **2a** from 3,4-bis{6-[4-(5-heptylpyrimidin-2-ly)phenyloxy]hexyloxy}benzoic acid (0.20 g, 0.23 mmol) and 1H,1H,2H,2H-heptadecafluoro-1-decanol (0.10 g, 0.23 mmol). Purification using column chromatography on silica gel with a toluene/ethyl acetate (8/1) mixture as eluent and reprecipitation with dichloromethane/ethanol (1/8) gave the desired product: yield 0.12 g (40%) of a white solid. ^{1}H NMR (500 MHz, $CDCl_3$) δ_H/ppm: 8.56 (s, 4H, Ar-**H**), 8.33 (d, 4H, Ar-**H**, $J = 9.2$ Hz), 7.64 (dd, 1H, Ar-**H**, $J = 8.3$ Hz, 1.7 Hz), 7.53 (d, 1H, Ar-**H**, $J = 1.7$ Hz), 6.96 (d, 4H, Ar-**H**, $J = 8.6$ Hz), 6.88 (d, 1H, Ar-**H**, $J = 8.6$ Hz), 4.60 (t, 2H, -COOC**H$_2$**-, $J = 6.3$ Hz), 4.07 (t, 2H, -OC**H$_2$**-, $J = 6.9$ Hz), 4.06 (t, 2H, -OC**H$_2$**-, $J = 6.9$ Hz), 4.02 (t, 4H, -OC**H$_2$**-, $J = 6.3$ Hz), 2.65-2.55 (m, 6H, aliphatic-**H**), 1.91–1.83 (m, 8H, aliphatic-**H**), 1.66–1.55 (m, 12H, aliphatic-**H**), 1.34–1.27 (m, 16H, aliphatic-**H**), 0.88 (t, 6H, -C**H$_3$**, $J = 7.2$ Hz); IR (KBr) ν_{max}/cm^{-1}: 2939, 2857, 1717, 1612, 1584, 1270, 1146, 1213 cm^{-1}. Elemental analysis, calculated for $C_{63}H_{73}N_4O_6F_{17}$: C, 57.97%; H, 5.64%; N, 4.29%. Found: C, 57.61%; H, 5.42%; N: 4.19%.

*2.2.6 1H,1H,2H,2H-Heptadecafluoro-1-decyl 3,4,5-tris{6-[4-(5-heptylpyrimidin-2-ly)phenyloxy]hexyloxy}benzoate, (**2c**)*

Synthesised using the same method as that used for compound **2a** from 3,4,5-tris{6-[4-(5-heptylpyrimidin-2-ly)phenyloxy]hexyloxy}benzoic acid (0.38 g, 0.30 mmol) and 1H,1H,2H,2H-heptadecafluoro-1-decanol (0.14 g, 0.30 mmol). Purification using column chromatography on silica gel with a toluene/ethyl acetate mixture (5/1) as eluent and reprecipitation with dichloromethane/ethanol (1/6) gave the desired product: yield 0.19 g (38%) of a white solid. ^{1}H NMR (400 MHz, $CDCl_3$) δ_H/ppm: 8.56 (s, 4H, Ar-**H**), 8.55 (s, 2H, Ar-**H**), 8.34–8.31 (m, 6H, Ar-**H**), 7.26 (s, 2H, Ar-**H**), 6.97–6.94 (m, 6H, Ar-**H**), 4.60 (t, 2H, -COOC**H$_2$**-, $J = 6.6$ Hz), 4.06–3.98 (m, 12H, -OC**H$_2$**-), 2.66–2.56 (m, 8H, aliphatic-**H**), 1.90–1.75 (m, 12H, aliphatic-**H**), 1.65–1.56 (m, 18H, aliphatic-**H**), 1.34–1.26 (m, 24H, aliphatic-**H**), 0.88 (t, 9H, -C**H$_3$**, $J = 7.2$ Hz); IR (KBr) ν_{max}/cm^{-1}: 2929, 2857, 1719, 1608, 1586, 1252, 1120, 1216 cm^{-1}. Elemental analysis, calculated for $C_{86}H_{105}N_6O_8F_{17}$: C, 61.37%; H: 4.59%; N: 2.90%. Found: C, 61.69%; H, 4.80%; N, 2.86%.

*2.2.7 Decyl 4-{6-[4-(5-heptylpyrimidin-2-ly)phenyloxy]hexyloxy}benzoate, (**3a**)*

To a solution of 4-{6-[4-(5-heptylpyrimidin-2-ly)phenyloxy]hexyloxy}benzoic acid (0.28 g, 0.58 mmol) and 1-decanol (0.093 g, 0.59 mmol) in dichloromethane (20 ml), we added *N, N'*-dicyclohexylcarbodiimide (0.16 g, 0.76 mmol) and 4-(*N, N*-dimethylamino)pyridine (0.093 g, 0.76 mmol). The resulting solution was stirred at room temperature for 21 h. Precipitated materials were removed by filtration. After removal of the solvent by evaporation, the residue was purified using column chromatography on silica gel with dichloromethane as eluent. Recrystallisation from an ethanol/ethyl acetate (3/1) mixture gave the desired product: yield 0.25 g (77%) of a white solid. ^{1}H NMR (500 MHz, $CDCl_3$) δ_H/ppm: 8.57 (s, 2H, Ar-**H**), 8.34 (d, 2H, Ar-**H**, $J = 8.6$ Hz), 7.98 (d, 2H, Ar-**H**, $J = 8.6$ Hz), 6.98 (d, 2H, Ar-**H**, $J = 9.2$ Hz), 6.90 (d, 2H, Ar-**H**, $J = 8.6$ Hz), 4.27 (t, 2H, -COOC**H$_2$**, $J = 6.6$ Hz), 4.05 (t, 2H, -OC**H$_2$**, $J = 6.3$ Hz), 4.03 (t, 2H, -OC**H$_2$**, $J = 6.6$ Hz), 2.59 (t, 2H, Ar-C**H$_2$**, $J = 7.7$ Hz), 1.86–1.84 (m, 4H, aliphatic-**H**), 1.74 (qui, 2H, aliphatic-**H**, $J = 6.9$ Hz), 1.64 (qui, 2H, aliphatic-**H**, $J = 7.4$ Hz), 1.57 (qui, 4H, aliphatic-**H**, $J = 3.7$ Hz), 1.42 (qui, 2H, aliphatic-**H**, $J = 7.5$ Hz), 1.34–1.27 (m, 20H, aliphatic-**H**), 0.88(t, 6H, -C**H$_3$**, $J = 6.9$ Hz); IR (KBr) ν_{max}/cm^{-1}: 2928, 2857, 1710, 1606, 1583, 1256, 1162 cm^{-1}. Elemental analysis, calculated for $C_{40}H_{58}N_2O_4$: C, 76.15%; H: 9.27%; N: 4.44%. Found: C, 75.94%; H, 9.38%; N, 4.35%.

*2.2.8 Decyl 3,4-bis{6-[4-(5-heptylpyrimidin-2-ly)phenyloxy]hexyloxy}benzoate, (**3b**)*

Synthesised using the same method as that used for compound **2a** from 3,4-bis{6-[4-(5-heptylpyrimidin-2-ly)phenyloxy]hexyloxy}benzoic acid (0.18 g, 0.21 mmol) and 1-decanol (35 mg, 0.22 mmol). Purification using column chromatography on silica gel with a toluene/ethyl acetate (7/1) mixture as eluent and reprecipitation with dichloromethane/ethanol (1/6) gave the desired product: yield 0.11 g (53%) of a white solid. ^{1}H NMR (500 MHz, $CDCl_3$) δ_H/ppm: 8.56 (s, 4H, Ar-**H**), 8.33 (d, 4H, Ar-**H**, $J = 9.2$ Hz), 7.64 (dd, 1H, Ar-**H**, $J = 8.3$ Hz, 1.7 Hz), 7.55 (d, 1H, Ar-**H**, $J = 1.7$ Hz), 6.96 (d, 4H, Ar-**H**, $J = 8.0$ Hz), 6.87 (d, 1H, Ar-**H**, $J = 8.6$ Hz), 4.28 (t, 2H, -COOC**H$_2$**-, $J = 6.9$ Hz), 4.07 (t, 4H, -OC**H$_2$**-, $J = 6.6$ Hz), 4.02 (t, 4H, -OC**H$_2$**-, $J = 6.6$ Hz), 2.59 (t, 4H, Ar-C**H$_2$**-, $J = 7.7$ Hz), 1.90–1.83 (m, 8H, aliphatic-**H**), 1.75 (qui, 2H, aliphatic-**H**, $J = 7.0$ Hz), 1.63 (qui, 4H, aliphatic-**H**, $J = 7.5$ Hz), 1.58–1.56 (m, 12H, aliphatic-**H**), 1.43 (qui, 2H, aliphatic-**H**, $J = 7.3$ Hz), 1.38–1.27 (m, 28H, aliphatic-**H**), 0.90-0.86 (m, 9H, -C**H$_3$**); IR (KBr) ν_{max}/cm^{-1}: 2925, 2855, 1710, 1610, 1588, 1268, 1168 cm^{-1}.

*2.2.9 Decyl 3,4,5-tris{6-[4-(5-heptylpyrimidin-2-ly)phenyloxy]hexyloxy}benzoate, (**3c**)*

Synthesised using the same method as that used for compound **3a** from 3,4,5-tris{6-[4-(5-heptylpyrimidin-2-ly)phenyloxy]hexyloxy}benzoic acid (0.25 g, 0.20 mmol) and 1-decanol (32 mg, 0.20 mmol). Purification using column chromatography on silica gel using a toluene/ethyl acetate (7/1) mixture as eluent and reprecipitation with dichloromethane/ethanol (1/7) gave the desired product: yield 0.17 g (64%) of a white solid. ^{1}H NMR (500 MHz, $CDCl_3$) δ_H/ppm: 8.56 (s, 4H, Ar-**H**), 8.55 (s, 2H, Ar-**H**), 8.34–8.31 (m, 6H, Ar-**H**), 7.27 (s, 2H, Ar-**H**), 6.98–6.94 (m, 6H, Ar-**H**), 4.29 (t, 2H, -COOC**H$_2$**-, $J = 6.9$ Hz), 4.06–3.98 (m, 12H, -OC**H$_2$**-), 2.60–2.56 (m, 6H, Ar-C**H$_2$**-), 1.90–1.73 (m, 14H, aliphatic-**H**), 1.66–1.50 (m, 16H, aliphatic-**H**), 1.44–1.27 (m, 40H, aliphatic-**H**), 0.89-0.85 (m, 12H, -C**H$_3$**); IR (KBr) ν_{max}/cm^{-1}: 2925, 2853, 1711, 1607, 1585, 1249, 1167 cm^{-1}.

2.3 Liquid-crystalline and physical properties

The initial phase assignments and corresponding transition temperatures for the final products were determined using thermal optical microscopy with a polarising microscope (Optiphoto POL; Nikon Corp., Tokyo, Japan) equipped with a Mettler FP82 microfurnace and FP80 control unit. The heating and cooling rates were 5°C min^{-1}. Temperatures and

enthalpies of transition were investigated using differential scanning calorimetry (DSC) using a Seiko DSC 6200 calorimeter. The materials were studied at a scanning rate of 5°C min^{-1}, for both heating and cooling cycles, after being encapsulated in aluminium pans. The X-ray diffraction (XRD) patterns of the homeotropically aligned samples on cooling processes were obtained using a real-time X-ray diffractometer (D8 Discover; Bruker AXS GmbH, Karlsruhe, Germany) equipped with a hot stage and a temperature-control processor. A sample was put on a convex lens coated with surfactant for homeotropic alignment, which was placed in a custom-made temperature stabilised holder (stability within ± 0.1°C). The textural observations were performed by polarised light microscopy using a CCD camera. The X-ray apparatus was equipped with a cross-coupled Göbel mirror on a platform system with a two-dimensional position-sensitive proportional counter (PSPC) detector (HI-Star; Bruker AXS GmbH). X-rays were generated at 45 kV and 20 mA; a parallel Cu Kα X-ray beam was used to irradiate the sample. Each diffraction pattern was obtained using the PSPC detector at a camera distance of 150 mm. The phase transition of the sample under the X-ray beam was monitored by observing the texture using a CCD camera. We also confirmed that any degradation of the sample did not take place under the X-ray beam.

3. Results and discussion

3.1 Phase transition properties

Transition temperatures and transition enthalpies of the amphiphilic oligomers **2a**–**2c** determined using polarised optical microscopy (POM) and DSC are presented in Table 1.

Compound **2a**, with one phenylpyrimidine moiety, showed the phase sequence Iso–SmC–Cry. The SmC phase was identified by a broken fan texture in the planarly aligned region and a Schlieren texture in the homeotropically aligned region. Compound **2b**, possessing two phenylpyrimidine moieties, showed the phase sequence Iso–SmA–Cry. The SmA phase showed a fan

Table 1. Transition temperatures (°C) and transition enthalpies (kJ mol^{-1}, in brackets) for compounds **2a**–**2c**.

Compounds	Cry	Col	SmC	SmA	I
2a	• 113.8 (31.2)		• 158.3 (16.6)		•
2b	• 101.7 (38.6)			• 149.3 (19.7)	•
2c	• 93.7 (72.7)	• 86.2 (6.3)		• 107.6 (5.4)	•

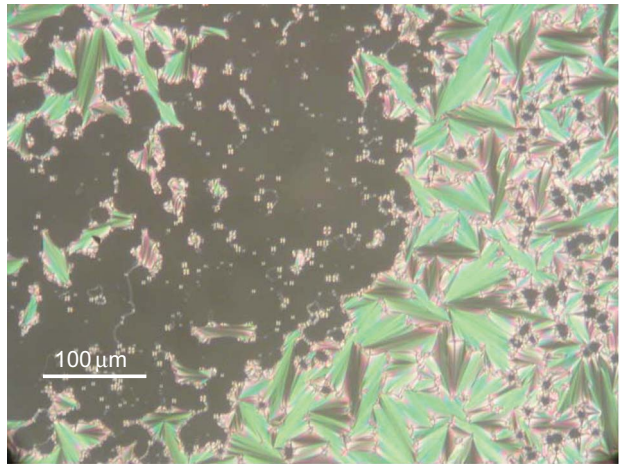

Figure 4. Optical texture of the SmA phase of compound **2b** at 140°C (colour version online).

texture in the planarly aligned region and a completely dark texture in the homeotropically aligned region as portrayed in Figure 4. Compound **2c**, possessing three phenylpyrimidine moieties, showed the phase sequence Iso–SmA–Col–Cry. Figure 5 shows optical textures of the SmA and Col phases. In the SmA–Col phase transition, the fans of the SmA phase were broken slowly; a weakly birefringent fan texture was observed in the Col phase. Compounds **2a**–**2c** show a phase sequence SmC–SmA–Col when the number of phenylpyrimidine moieties is increased. Marked differences exist in phase sequence between compounds **1a**–**1c** and compounds **2a**–**2c**. Furthermore, compounds **2a**–**2c** showed no glassy state, although compounds **1b** and **1c** exhibited it.

To clarify effects of the semiperfluorinated alkyl chain on the phase transition behaviour, we prepared oligomers **3a**–**3c** possessing a hydrocarbon alkyl chain instead of the semiperfluorinated chain (Figure 6). Their transition temperatures and transition enthalpies, determined by POM and DSC, are presented in Table 2.

Compounds **3a**–**3c** show typical calamitic phases of thermotropic liquid crystals. When the number of phenylpyrimidine moieties is increased, the smectic phases are destabilised. Compound **3c** shows only a nematic phase. The excluded volume effect induced by the shape amphiphilicity is dominant for the phase formation of compounds **3a**–**3c**.

3.2. Phase structures

Figure 7 shows an X-ray diffraction intensity profile in the small angle region of compound **2b** in the SmA phase at 133°C. Two weak diffractions exist at $2\theta =$ 2.10° and 4.26°, respectively corresponding to the spacings of 42.0 Å and 20.7 Å. The 2D pattern of the sample

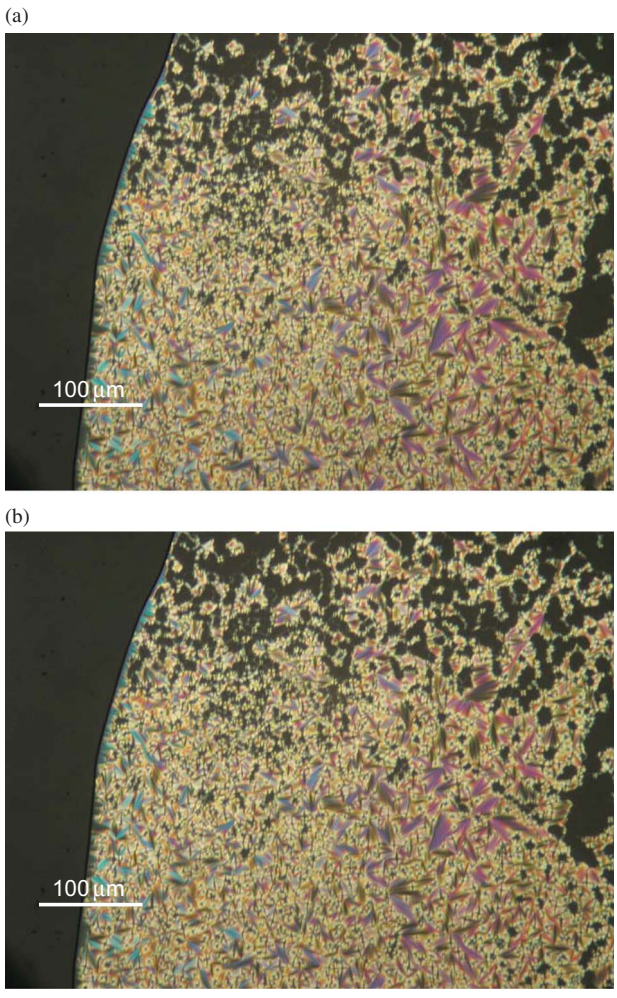

Figure 5. Optical textures of (a) the SmA phase at 110°C and (b) the Col phase at 80°C for compound **2c** (colour version online).

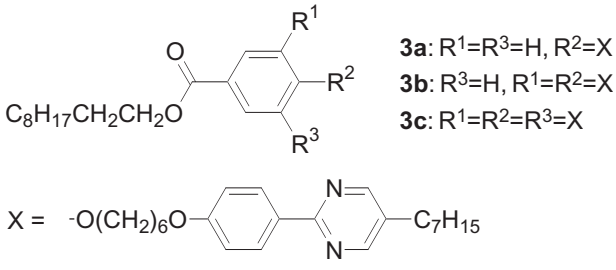

Figure 6. Molecular structures of compounds **3a**–**3c**.

in the SmA phase shows that two reflection peaks in the small angle region are positioned in one direction (Figure 8). Figure 9 presents the expected molecular conformation using MOPAC (MOPAC-6/PM3). The molecular length is estimated to be 44 Å. The SmA phase is thought to have a monolayered structure as

Table 2. Transition temperatures (°C) and transition enthalpies (kJ mol^{-1}, in brackets) for compounds **3a**–**3c**.

Compounds	Cry	SmC	SmA	N	I
3a	• 75.0 (48.6)	• 91.4 (–[a])	• 99.2 (19.8)		•
3b	• 77.0 (39.8)	• 66.0 (–[a])	• 88.6 (4.4)	• 90.9 (7.8)	•
3c	• 93.9 (85.1)			• 75.2 (1.8)	•

Note: [a]Smaller than the detection limit.

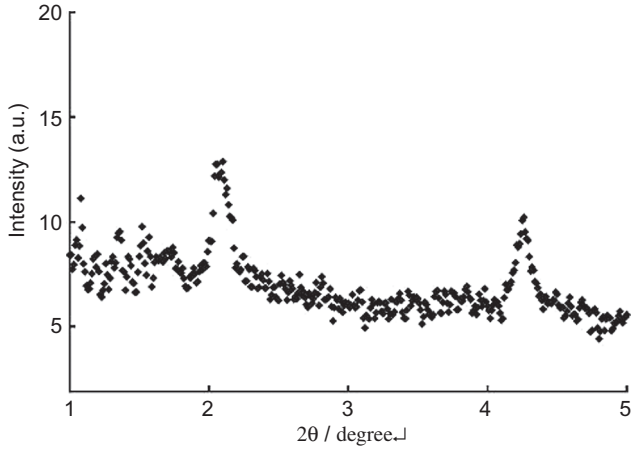

Figure 7. X-ray diffraction intensity profile in the small angle region of compound **2b** in the SmA phase at 133°C.

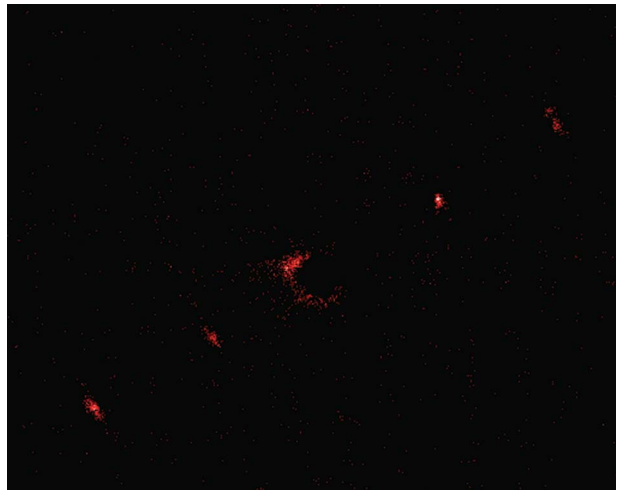

Figure 8. X-ray diffraction pattern of compound **2b** in the SmA phase at 133°C (colour version online).

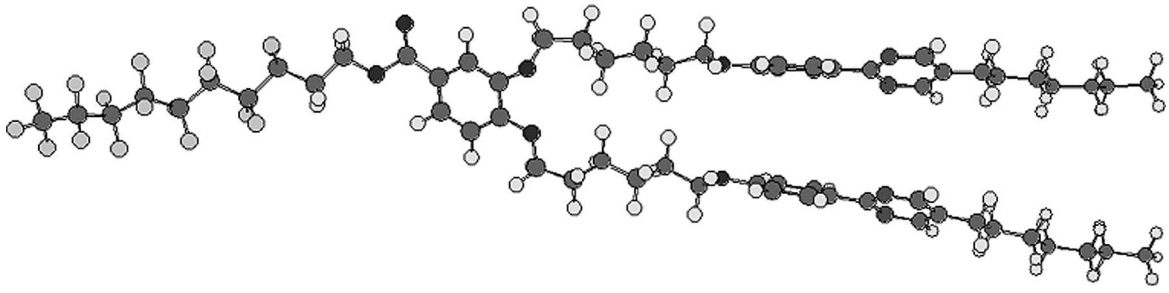

Figure 9. MOPAC model for the expected molecular conformation of compound **2b**.

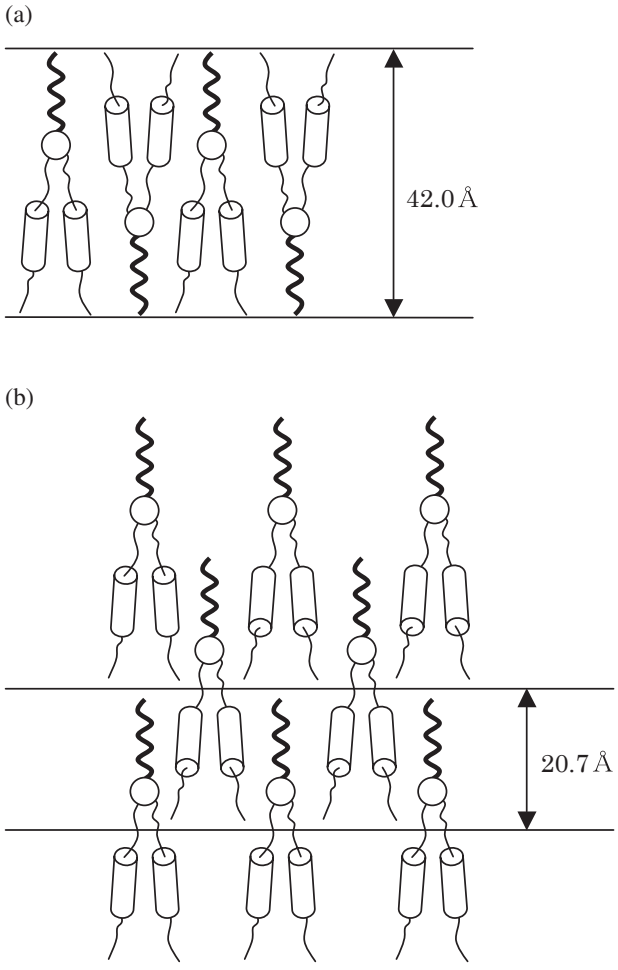

Figure 10. Possible molecular arrangement in the SmA phase of compound **2b**.

shown in Figure 10(a). However, intensity of each peak was unusually weak. Some examples of observations of two reflections of the small-angle region were reported in the modulated SmA phases [27–29] and the incommensurate SmA phases [30–34]. At present we cannot exclude the possibility that the SmA phase is an incommensurate phase in which two periodic density waves co-exist along the layer normal. If this is the case, the monolayered structure (Figure 10(a)) and the intercalated structure (Figure 10(b)) might co-exist in the incommensurate SmA phase. Whether the SmA phase of compound **2b** is a monolayer SmA phase or an incommensurate SmA phase, the steric effect organised by the shape amphiphilicity is dominant for the formation of the SmA phase. On the other hand, compound **1b** reportedly forms bilayer SmA and Col phases, which are stabilised by the segregation effect of the semiperfluorinated chain.

Figure 11 shows X-ray diffraction intensity profiles in the small angle region of compound **2c** in the SmA and Col phases. Figure 12 shows the 2D patterns of the sample in both phases. In the SmA phase at 95°C, a diffraction at $2\theta = 2.03°$ was observed in the small angle region, corresponding to a spacing of 43.5 Å. The molecular length was estimated to be about 44 Å for the extended structure using MOPAC (MOPAC-6/PM3). Therefore the SmA phase has a monolayered structure as shown in Figure 13(a). In the Col phase at 75°C, three reflections were observed – $2\theta = 1.47°$, $1.70°$ and $2.93°$ – which can be indexed based on a rectangular 2D lattice with lattice parameters of $a = 120.2$ Å and $b = 57.6$ Å, as shown in Table 3. Figure 13(b) shows a possible arrangement of the molecules in the columnar phase. In the columnar phase, the fluid fluorinated alkyl chains are segregated in the central region of each column, surrounded by the outer region composed of the aliphatic spacers and phenylpyrimidine mesogenic cores. The inter-column regions comprise the flexible aliphatic alkyl chains.

Compound **1c** exhibits a bilayer SmA–Cub_v phase transition, whereas compound **2c** shows a monolayer SmA–Col_r phase transition. On the other hand, compound **3c** shows only a nematic phase. A steric effect attributable to the taper shape gives rise to a nematic phase and/or a monolayer smectic phase. A segregation

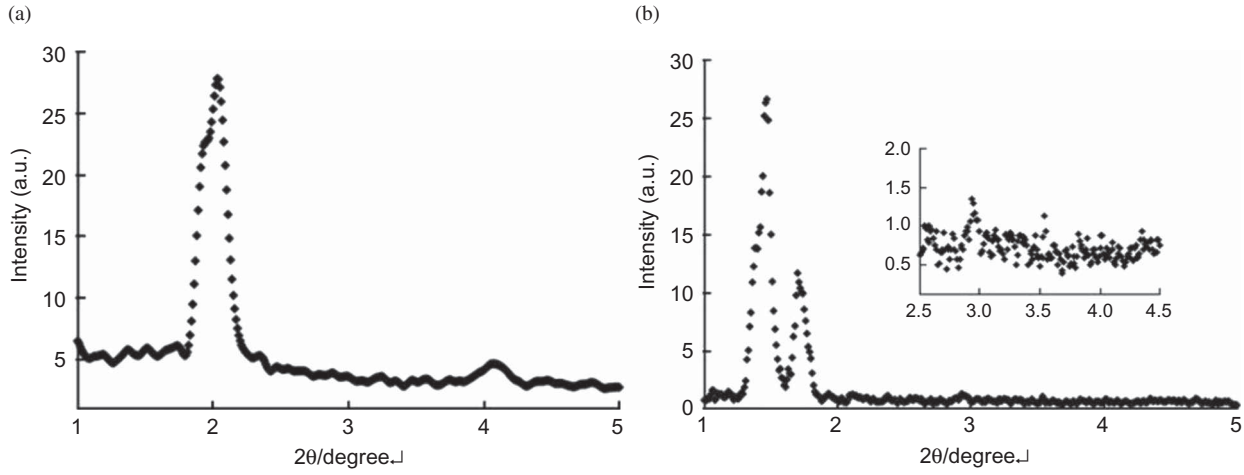

Figure 11. X-ray diffraction intensity profiles of compound **2c** in (a) the SmA phase at 95°C and (b) the Col phase at 75°C; an expansion is included for clarity.

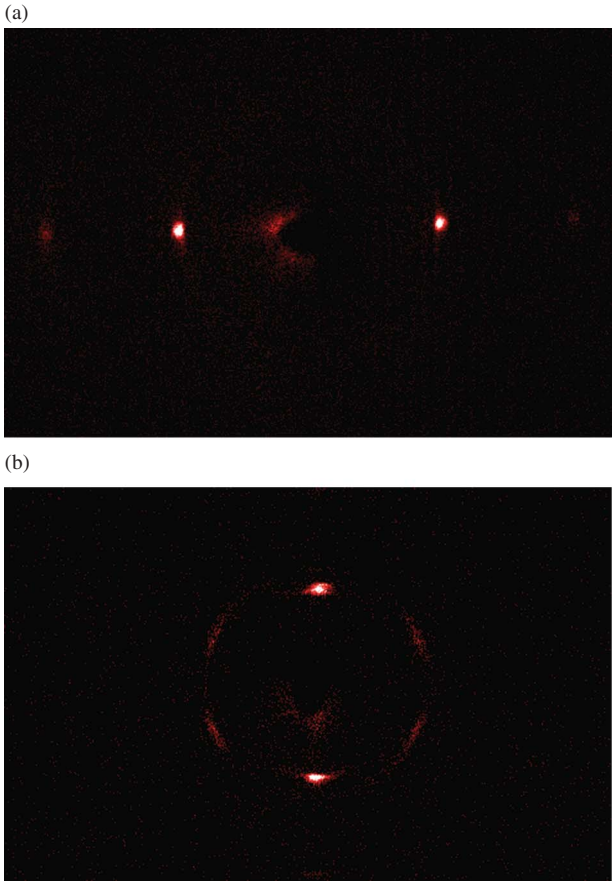

Figure 12. X-ray diffraction patterns of compound **2c** in (a) the SmA phase at 95°C and (b) the Col phase at 75°C (colour version online).

effect attributable to incompatibility between semiperfluorinated chains and mesogenic moieties plays an important role in the appearance of a bilayer SmA and/or a Col phase. Competition of two different molecular packings for compound **1c**, the steric and segregation effects, might give rise to the fluctuated bilayer SmA phase, which organises the lamellar to a bicontinuous cubic phase transition. On the other hand, compound **2c** induces the entropy-driven monolayered structure and the enthalpy-driven columnar structure. The monolayer SmA-to-Col phase transition is thought to occur via change in driving force of the mesophase formation from shape incompatibility to hydrocarbon–fluorocarbon incompatibility.

Table 3. Observed reflections in the columnar phase of compound **2c**.

θ_{exp} (deg)	*h k l*	$\theta_{calcd.}$ (deg)
0.735	110	0.735
0.850	200	0.850
1.465	220	1.470

4. Conclusions

In summary, the newly designed amphiphilic oligomers were found to exhibit the phase sequence SmC–SmA–Col_r with increasing phenylpyrimidine mesogenic moieties. Compound **2c**, possessing a semiperfluorinated chain and three mesogenic moieties, exhibits monolayer SmA and Col_r phases. Introduction of the amphiphilic characters, i.e. shape incompatibility and hydrocarbon–fluorocarbon incompatibility, into a pre-organised oligomer produces a phase transition from an entropy-driven monolayer SmA phase to an enthalpy-driven Col_r phase.

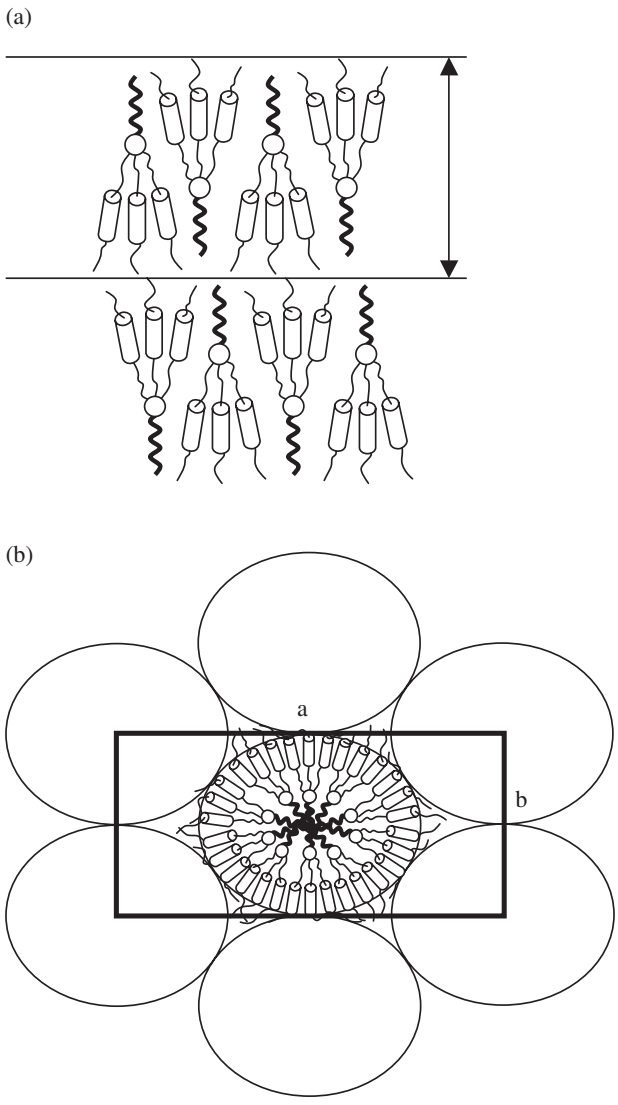

Figure 13. Arrangements suggested for compound **2c** in (a) the monolayer SmA phase with a layer spacing of 43.5 Å and (b) the rectangular columnar phase with lattice parameters of $a = 120.2$ Å and $b = 57.6$ Å.

Acknowledgement

This work was partially supported by a Grant for Hirosaki University Institutional Research.

References

[1] Goodby, J.W.; Mehl, G.H.; Saez, I.M.; Tuffin, R.P.; Mackenzie, G.; Auzely Velty, R.; Benvegu, T.; Plusquellec, D. *Chem. Commun.* **1998**, 2057–2070.
[2] Goodby, J.W.; Saez, I.M.; Cowling, S.J.; Görtz, V.; Draper, M.; Hall, A.W.; Sia, S.; Cosquer, G.; Lee, S.-E.; Raynes, E.P. *Angew. Chem., Int. Ed.* **2008**, *47*, 2754–2787.
[3] Tschierske, C. *J. Mater. Chem.* **1998**, *8*, 1485–1508.
[4] Tschierske, C. *J. Mater. Chem.* **2001**, *11*, 2647–2671.
[5] Tschierske, C. *Chem. Soc. Rev.* **2007**, *36*, 1930–1970.
[6] Kato, T. *Science* **2002**, *295*, 2414–2418.
[7] Kato, T.; Mizoshita, N.; Kishimoto, K. *Angew. Chem., Int. Ed.* **2006**, *45*, 38–68.
[8] Imrie, C.T.; Henderson, P.A. *Chem. Soc. Rev.* **2007**, *36*, 2096–2124.
[9] Lim, Y.-B.; Moon, K.-S.; Lee, M. *J. Mater. Chem.* **2008**, *18*, 2909–2918.
[10] Yoshizawa, A. *J. Mater. Chem.* **2008**, *18*, 2877–2889.
[11] Nguyen, H.-T.; Destrade, C.; Malthete, J. *Adv. Mater.* **1997**, *9*, 375–388.
[12] Donnio, B.; Buathong, S.; Bury, I.; Guillon, D. *Chem. Soc. Rev.* **2007**, *36*, 1495–1513.
[13] Ponimarenko, S.A.; Boko, N.I.; Shibaev, V.P. *Polym. Sci., Ser. C* **2001**, *43*, 1–45.
[14] Paleos, C.M.; Tsiourvas, D. *Liq. Cryst.* **2001**, *28*, 1127–1161.
[15] Donnio, B.; Guillon, D.; Deschenaux, R.; Bruce, D.W.; In *Comprehensive Coordination Chemistry II*: McCleverty, J.A., Meyer, T.J., Fujita, M., Powell, A., Creutz, C., Eds.; Elsevier: Oxford, 2003; Chapter 7.9, pp 357–627.
[16] Pelzl, G.; Diele, S.; Weissflog, W. *Adv. Mater.* **1999**, *11*, 707–724.
[17] Reddy, R.A.; Tschierske, C. *J. Mater. Chem.* **2006**, *16*, 907–961.
[18] Ryu, J.-H.; Lee, M. *Struc. Bond* **2008**, *128*, 63–98.
[19] Demus, D. In *Handbook of Liquid Crystals*; Demus, D., Goodby, J.W., Gray, G.W., Spiess, H.-W., Vill, V., Eds.; Wiley-VCH: Weinheim, 1998; Vol. 1, pp 133–187.
[20] Goodby, J.W. In *Handbook of Liquid Crystals*; Demus, D., Goodby, J.W., Gray, G.W., Spiess, H.-W., Vill, V., Eds.; Wiley-VCH: Weinheim, 1998; Vol. 2A, pp 3–21.
[21] Giroud-Godquin, A.M. In *Handbook of Liquid Crystals*; Demus, D., Goodby, J.W., Gray, G.W., Spiess, H.-W., Vill, V., Eds.; Wiley-VCH: Weinheim, 1998; Vol. 2B, pp 901–932.
[22] Bruce, D.W. In *Inorganic Materials*; Bruce, D.W., O'Hare, D., Eds.; Wiley: Chichester, 1992: pp 405–490.
[23] Praefcke, K.; Singer, D. In *Handbook of Liquid Crystals*; Demus, D., Goodby, J.W., Gray, G.W., Spiess, H.-W., Vill, V., Eds.; Wiley-VCH: Weinheim, 1998; Vol. 2B, pp 945–967.
[24] Kato, T. In *Handbook of Liquid Crystals*; Demus, D., Goodby, J.W., Gray, G.W., Spiess, H.-W., Vill, V., Eds.; Wiley-VCH: Weinheim, 1998; Vol. 2B, pp 969–979.
[25] Yamaguchi, A.; Maeda, Y.; Yokoyama, H.; Yoshizawa, A. *Chem. Mater.* **2006**, *18*, 5704–5710.
[26] Yamaguchi, A.; Yoshizawa, A. *Mol. Cryst. Liq. Cryst.* **2007**, *479*, 181–189.
[27] Sigaud, G.; Hardouin, F.; Achard, M.F.; Levelut, A.M. *J. Phys. France* **1981**, *42*, 107–111.
[28] Prost, J.; Barois, P. *J. Chem. Phys.* **1983**, *80*, 65–81.
[29] Pocecha, D.; Kardas, D.; Gorecka, E.; Szydlowska, J.; Mieczkowski, J.; Guillon, D. *J. Mater. Chem.* **2003**, *13*, 34–37.
[30] Yamaguchi, A.; Nishiyama, I.; Yamamoto, J.; Yokoyama, H.; Yoshizawa, A. *J. Mater. Chem.* **2005**, *15*, 280–288.
[31] Yamaguchi, A.; Nishiyama, I.; Yamamoto, J.; Yokoyama, H.; Yoshizawa, A. *Mol. Cryst. Liq. Cryst.* **2005**, *439*, 85–95.
[32] Mang, J.T.; Cull, B.; Shi, Y.S.; Patel, P.; Kumar, S. *Phys. Rev. Lett.* **1995**, *74*, 4241–4244.
[33] Hardouin, F.; Achard, M.F.; Jin, J.L.; Shin, J.W.; Yun, Y.K. *J. Phys. II* **1994**, *4*, 627–643.
[34] Hardouin, F.; Achard, M.F.; Jin, J.L.; Shin, J.W.; Yun, Y.K. *J. Phys. II* **1995**, *5*, 927–935.